Chemical Science

EDGE ARTICLE

View Article Online
View Journal | View Issue

Cite this: *Chem. Sci.*, 2019, **10**, 11073

All publication charges for this article have been paid for by the Royal Society of Chemistry

Received 29th May 2019
Accepted 16th October 2019

DOI: 10.1039/c9sc02610j

rsc.li/chemical-science

Synthesis of montbretin A analogues yields potent competitive inhibitors of human pancreatic α-amylase†

Christina R. Tysoe,[a] Sami Caner,[b] Matthew B. Calvert,[a] Anna Win-Mason,[a] Gary D. Brayer[b] and Stephen G. Withers *[a]

Simplified analogues of the potent human amylase inhibitor montbretin A were synthesised and shown to bind tightly, $K_I = 60$ and 70 nM, with improved specificity over medically relevant glycosidases, making them promising candidates for controlling blood glucose. Crystallographic analysis confirmed similar binding modes and identified new active site interactions.

The healthcare burden of diabetes mellitus has steadily risen over the past century, with an increase from 108 million adult cases worldwide in 1980 to 422 million cases in 2014.[1] Strikingly, type II diabetes accounts for 90–95% of all cases.[2] The inhibition of carbohydrate catabolism has been explored as a means of mediating post-prandial blood glucose levels for the treatment of type II diabetes.[3] Targeting of carbohydrate catabolism provides two benefits: beyond directly modulating blood glucose levels it can also promote weight loss in pre-diabetic individuals to prevent the onset of diabetes. Miglitol, voglibose and acarbose are three inhibitors of carbohydrate catabolism that are currently in medical use. These compounds act as inhibitors of the mammalian gut α-glucosidases, thereby mediating post-prandial blood glucose levels.[4] While effective in preventing hyperglycemia, the resulting displacement of di- and tri-saccharides into the lower gut produces unwanted side effects arising from their strong osmotic effects within the large intestine and their rapid processing by anaerobic bacteria, resulting in diarrhea, nausea, and abdominal discomfort.[5]

Human pancreatic α-amylase (HPA) catalyzes the endo-hydrolysis of ingested starches into maltose and maltotriose[6] and its activity has been positively correlated with post-prandial blood glucose levels. Consequently the targeted inhibition of this enzyme has been highlighted as a means of managing post-prandial blood glucose levels while avoiding side effects associated with general α-glucosidase inhibition.[7] Most designs of glycosidase inhibitors have been based upon azasugar scaffolds in which a nitrogen atom replaces O5 or C1 of the sugar ring in the −1 binding site.[8] In this manuscript we explore a completely new pharmacophore for α-amylase inhibition involving stacked phenolic rings that interact closely with the conserved active site carboxylic acids. The parent molecule, montbretin A (MbA), is a complex flavonol glycoside produced by *Crocosmia crocosmiiflora* that acts as a potent and selective inhibitor of HPA ($K_I = 8$ nM).[9] This inhibitor has been tested in ZDF (Zucker diabetic fatty) rats and produced a significant decrease in blood glucose plasma levels, highlighting this compound as a promising lead for the therapeutic reduction of post-prandial blood glucose levels.[10] However its large-scale extraction and purification from the corms of *Crocosmia crocosmiiflora* is a challenging multistep process and requires a substantial amount of biomass. Consequently the design and synthesis of novel inhibitors based upon MbA's structure has been proposed as a means of generating chemically accessible structures of similar potency and specificity.[11]

Montbretin A contains a myricetin flavonol core glycosylated at the 3- and 4′-positions (Fig. 1a). The 3-OH is adorned with an α-linked D-glucopyranosyl-(β-1 → 2)-D-glucopyranosyl-(β-1 → 2)-L-rhamnopyranoside trisaccharide to which a 6-*O*-caffeic ester is attached on the central D-glucosyl group. The 4′-OH of myricetin bears a β-linked L-rhamnopyranosyl-(α-1 → 4)-D-xyloside. X-ray crystallographic analysis of MbA in complex with HPA showed notable points of contact occurring between the enzyme's catalytic residues and MbA's caffeic ester and

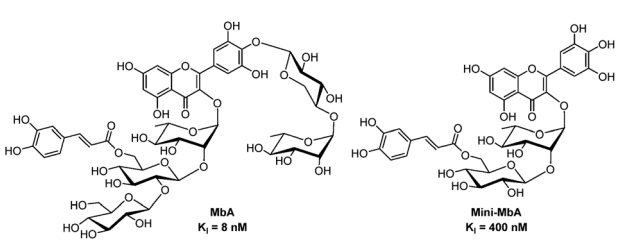

Fig. 1 Structures of montbretin A and mini-MbA.

[a]Department of Chemistry, University of British Columbia, 2036 Main Mall, Vancouver BC, Canada V6T 1Z1. E-mail: withers@chem.ubc.ca

[b]Department of Biochemistry and Molecular Biology, University of British Columbia, 2350 Health Sciences Mall, Vancouver BC, Canada V6T 1Z3

† Electronic supplementary information (ESI) available. See DOI: 10.1039/c9sc02610j

myricetin A-ring.[11] Meanwhile, minimal interactions were observed with the myricetin B-ring or any of MbA's carbohydrate appendages. Step-wise chemoenzymatic degradation of MbA had yielded a 'minimum inhibitory structure' termed mini-MbA (Fig. 1b). This inhibitor contained only the myricetin flavonol and caffeic acid linked through a D-glucopyranosyl-(β-1 → 2)-L-rhamnopyranose disaccharide, and had a K_I = 400 nM (ref. 12) towards HPA (lone myricetin and ethyl caffeate have K_I = 100 μM and 1.3 mM, respectively[9]). The retained potency of the simplified mini-MbA structure suggested that a suitable synthetic analogue could achieve equivalent levels of potency, thus mini-MbA was used as inspiration for our synthesis. It was not clear however, whether such a compound would retain the required specificity for HPA over the gut alpha-glucosidases given the active site similarities.

Quercetin was selected to replace myricetin as the flavonol core in our analogue synthesis since it, and its glycosylated derivatives, are substantially less expensive than other flavonols. Quercetin differs from myricetin only in hydroxylation of the B-ring and, as noted earlier, there are very few interactions between HPA and this ring.[13] In mini-MbA, the caffeic acid and myricetin groups are connected by a disaccharide, which forms a bridge of 7 atoms. This region formed no direct interactions with the enzyme, though it likely provides some conformational constraints. As a result, a variety of different chemical structures could be explored for the linker region. Requirements for linker length and rigidity could be assessed, as well as the possibility of incorporating new functionalities to create favorable interactions with the enzyme.

Quercetin-3-*O*-rutinoside was used as a convenient and inexpensive starting material for the synthesis since the pre-existing sugar at C3 could be used to differentiate the hydroxyls in a protecting group strategy. Quercetin-3-*O*-rutinoside was thus reacted with benzyl bromide in the presence of K_2CO_3, followed by cleavage of the 3-*O*-glycoside by treatment with HCl/ethanol to yield benzyl quercetin **2**, freeing the 3-OH for subsequent modification.[14] Analogues with simple linkers were first synthesized to test the basic concept of linking the two phenolics (Fig. 2). Optimal linker length and polarity was then explored through a series containing three, five, seven and eight atoms. Analogues **M01** to **M03** contained simple alkyl linkers of three, five and seven atoms long while **M04** contained a similarly flexible eight-atom triethylene glycol linker. Focus then changed to design of linkers that incorporate appropriate conformational constraints while seeking out favourable interactions of the side chains with active site residues. To that end analogues **M05** to **M11** were generated containing an amino acid linked to quercetin's 3-OH through a propyl chain (Scheme 1).

Tri-*O*-benzyl quercetin **2** was functionalized with 1-bromo-3-chloropropane, 1-bromo-5-chloropentane, 1-bromo-7-azidoheptane, or 1-bromo-8-azido-triethylene glycol depending on the analogue synthesized. Treatment with tetrabutylammonium azide produced a terminal azide, which was reduced with trimethylphosphine. In the cases of analogues **M01** to **M04**, this

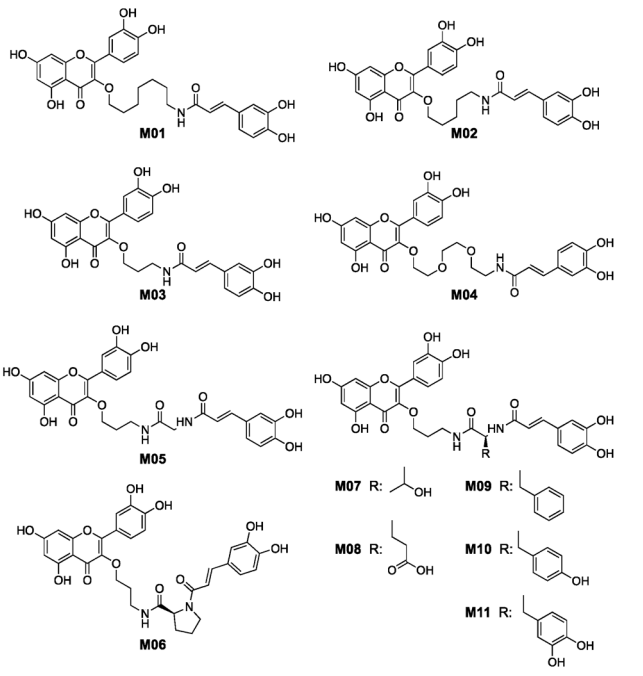

Fig. 2 Structures of synthetic MbA analogues.

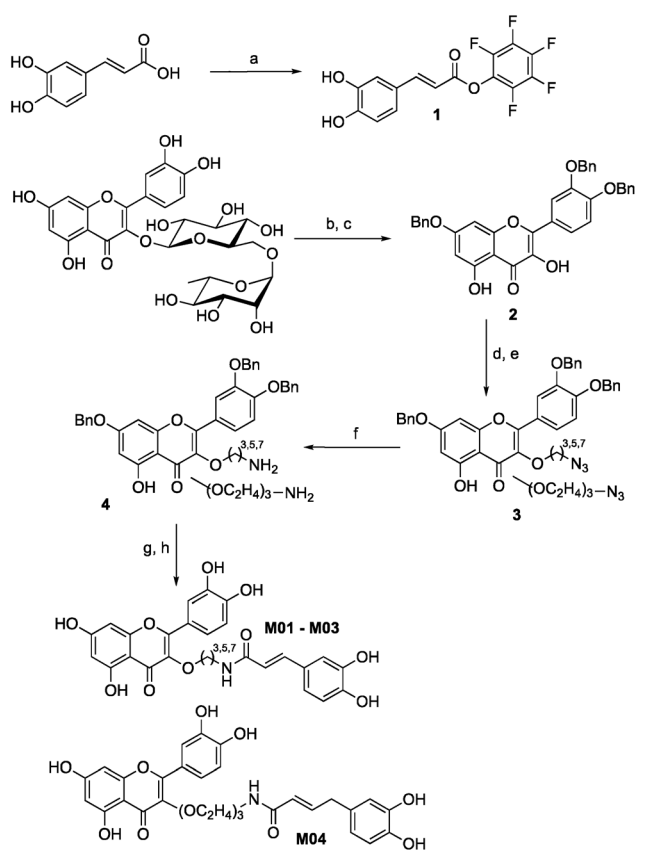

Scheme 1 Synthesis of analogues **M01** to **M04**: (a) PFP-TFA (1.2 equiv.), pyr (1.2 equiv.), DMF, 93%; (b) BnBr (5 equiv.), K_2CO_3 (5 equiv.), DMF, 70 °C, 18 h; (c) EtOH/HCl (20 : 1), 70 °C, 2 h 70% over two steps; (d) $Br(CH_2)_nCl$ or $Br(C_2H_4O)_2$ $C_2H_4N_3$ (1.5 equiv.), K_2CO_3 (1.5 equiv.), DMF/THF, 61–90% (e) $N(C_4H_9)_4N_3$ (2 equiv.), DMF, 50 °C, 90–95%; (f) PMe_3 (3 equiv.), THF/NaOH (0.05 M), 50–80%; (g) **1** (1 equiv.), pyr (1.5 equiv.), DCM/THF, 70%; (h) BBr_3 (7 equiv.), DCM, −78 °C, 7–16%.

could be coupled directly to caffeic acid through use of activated pentafluorophenyl caffeic ester **1**. For analogues **M05** to **M11**, the propylamine derivative **4 propyl** was coupled to one of six chosen Fmoc-L-amino acids (with appropriate side chain protecting groups) (Scheme 2).[15] The Fmoc group could be deprotected with 20% piperidine in dichloromethane followed by a second coupling with the pentafluorophenyl caffeic ester **1**. Deprotection of the benzyl ethers and amino acid protecting groups was achieved through treatment with BBr_3. While this synthesis allowed the construction of a small library of analogues, the final deprotection step in particular was prohibitively low yielding, posing a significant barrier to future applications. The continued study of any promising analogues required an improved synthesis, as will be explored below.

The eleven analogues were tested as inhibitors of HPA as shown in Table 1. Analogues **M01** and **M02** both had a $K_I = 4$ μM, demonstrating that joining the flavonol and caffeic acid groups with a simple linker could increase potency by 25 times compared to the lone flavonol ($K_I \sim 100$ μM).[9,13] However, these analogues were substantially less potent than mini-MbA, despite having the potential to form all the same interactions within the amylase active site. **M03** was no more potent than the lone flavonol, suggesting that its three-atom linker was too short to allow for proper orientation of the phenolic moieties in the active site. **M04**, which contained an eight-atom triethylene glycol-based linker (TEG), also failed to offer a significant increase in potency over the lone flavonol. Despite having a linker of similar length and flexibility to those of **M01** and **M02**, the incorporation of a triethylene glycol-based chain in place of a simple alkyl chain led to a 21-fold drop in potency, potentially due to the differences in polarity.

While amino acid based analogues **M05**, **M07**, and **M08** offered only meagre increases in potency compared to the lone flavonol, **M06** fared better with a $K_I = 1$ μM, perhaps due to the limited conformational range of its proline pre-organising the ligand for binding.

Introduction of aromatic residues into the linkers also afforded an increase in binding affinity. The phenylalanine-based analogue **M09** bound 22-fold tighter than the unfunctionalized glycine-based analogue **M05**, suggesting that its aromatic side chain likely creates favorable π stacking interactions in the active site, contributing 1.8 kcal mol^{-1} to binding affinity. Installation of hydroxyl groups onto the phenyl ring, as seen with the tyrosine-based analogue **M10** and the DOPA-based analogue **M11**, produced a further 40 to 47-fold increase in potency relative to **M09**, equating to a further ~2.5 kcal mol^{-1} contribution to the binding affinity. With inhibition constants of 70 and 60 nM, **M10** and **M11** bind approximately six times more tightly than the mini-MbA that inspired their synthesis. Thus not only have we replicated the affinity of the natural product with a simple, synthetically accessible analogue, but also we have substantially improved upon its binding affinity.

Table 1 Kinetic analysis of MbA analogues

MbA analogue	Linker	K_I against HPA (μM)
Quercetin/myricetin	—	~100
M01	Heptylene	4.2 ± 0.8
M02	Pentylene	4.0 ± 0.4
M03	Propylene	110 ± 10
M04	TEG	90 ± 20
M05	Gly	60 ± 10
M06	Pro	1.0 ± 0.1
M07	Thr	50 ± 10
M08	Glu	34 ± 5
M09	Phe	2.8 ± 0.4
M10	Tyr	0.07 ± 0.01
M11	DOPA	0.06 ± 0.02

To gain insights into the binding modes of the best of these analogues, and particularly to understand the greatly improved affinity of **M10** and **M11**, X-ray crystallographic analysis of analogues **M06** and **M10** in complex with HPA was pursued. The resulting crystal structures (PDBs 6OCN and 6OBX at 1.15 and 1.30 Å resolution) revealed the analogues in non-covalent complex within the enzyme active site. Importantly, an overlay of the **M06**/HPA and **M10**/HPA structures with that of mini-MbA/HPA showed essentially complete overlap of the flavonol and caffeic acyl moieties in each case, simplifying future design (Fig. 3a).

Proline-containing analogue **M06** created all of the polar contacts within the HPA active site that were previously observed with mini-MbA (Fig. 3b). Hydrogen bonding was observed between the caffeic acid catechol and R195, D197 and E233 of the enzyme. The 7-OH of **M06**'s flavonol formed hydrogen bonds with D197 and H201. A hydrogen bond was also observed between the C4 carbonyl of the flavonol and the side chain of T163. Meanwhile, the 3′-OH of the flavonol formed a hydrogen bond with the side chain of H201, as was also observed in the mini-MbA/HPA complex. This indicates that the more cost-effective quercetin was sufficient to form the necessary interactions within the active site. The absence of this 4′-*O*-disaccharide on mini-MbA opens this position up for hydrogen bonding with K200 in the active site, an interaction that is also seen with **M06**. In addition to these polar contacts, a π–CH stacking interaction appears to form between the proline side chain of **M06** and W59 of the enzyme.

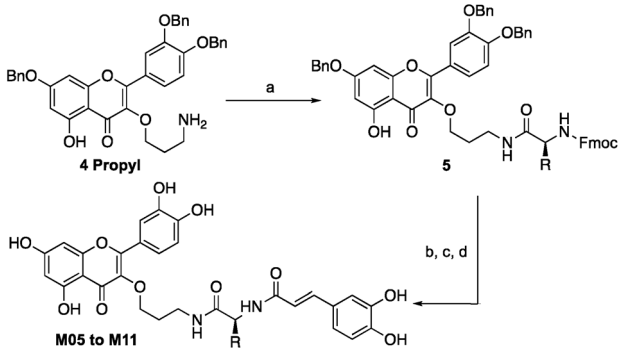

Scheme 2 Synthesis of analogues **M05** to **M11**: (a) Fmoc-L-Xaa-pfp (1 equiv.), pyr (1 equiv.), DCM, 75–90%; (b) 20% piperidine/DCM, 1 h; (c) **1** (1 equiv.), pyr (1.5 equiv.), THF/DCM, 50–75%; (d) BBr_3 (7 equiv.), DCM, −78 °C, 5–25%.

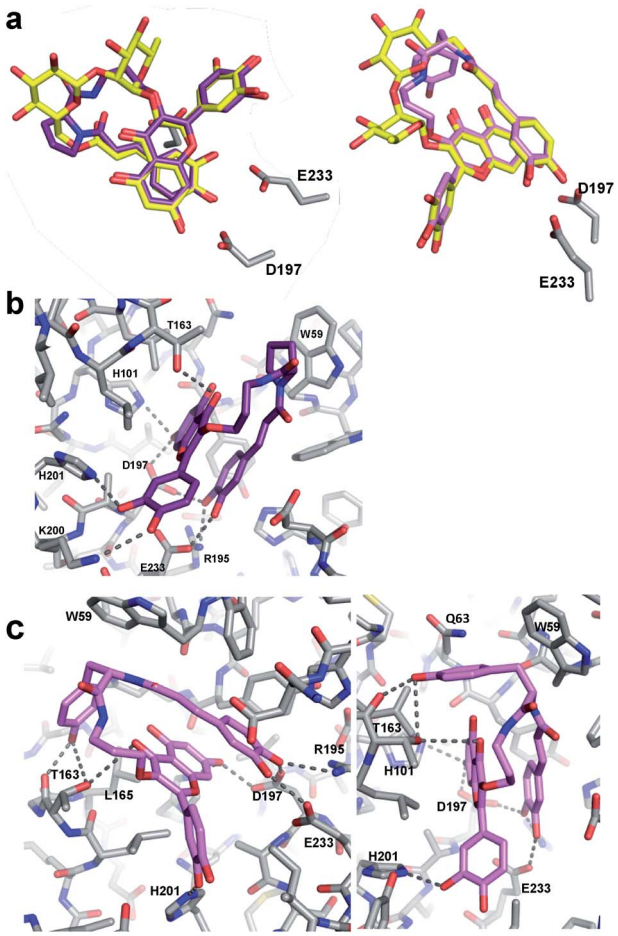

Fig. 3 X-ray crystal structures of **M06**/HPA and **M10**/HPA complexes. (a) Overlays of **M06** (purple) and **M10** (pink) with mini-MbA (yellow) show very similar placement of flavonol and catechol groups. (b) Interactions between **M06** (purple) and residues at the HPA active site (grey). Hydrogen bonds are shown as dashed lines. Polar interactions occurred between the flavonol and catechol of **M06** and the enzyme. (c) Two different views of the interactions between **M10** (pink) and residues of the HPA active site (grey). In addition to the polar contacts formed with the analogue flavonol and catechol, polar contacts occurred between the linker tyrosine and T163 of the enzyme. π-based interactions also occurred between the enzyme and aromatic tyrosine side chain.

Despite its high degree of alignment and reproducibility of polar contacts, **M06** is still 2.5 times less potent than mini-MbA, highlighting the importance of MbA's glycosidic appendages in stabilization of a pre-stacked conformation.

Analogue **M10** also formed all of the same hydrogen bonds within the amylase active site previously observed for mini-MbA and **M06** (Fig. 3c). In addition, and presumably largely responsible for its affinity enhancement, the tyrosine of **M10**'s linker formed hydrogen bonds with the main chain carbonyl and side chain hydroxyl of T163. These are accompanied by a number of CH–π–interactions between the tyrosine side chain and residues W59, Q63, and L165 of the enzyme.

To probe its specificity towards HPA, **M10** was tested as an inhibitor of ten other glycosidases, including human

Table 2 Specificity analysis of **M10**

Enzyme	**M10** IC_{50} (μM)
Roseburia inulivorans amylase A	NI
Butyrivibrio fibrisolvens amylase B	NI
Homo sapiens maltase-glucoamylase	NI
H. sapiens C-term sucrase-isomaltase	NI
Saccharomyces cerevisiae α-glucosidase	10.5 ± 0.7
Agrobacterium β-glucosidase	35.4 ± 5.7
Green coffee bean α-galactosidase	NI
E. coli β-galactosidase	NI
Jack bean α-mannosidase	NI

intestinal maltase-glucoamylase and sucrase-isomaltase, and two intestinal bacterial α-amylases (Table 2). The analogue showed no inhibitory activity towards these α-glucosidases at a concentration over 100-fold higher than its K_I value for HPA. **M10** did show some inhibitory activity against the non-relevant *S. cerevisiae* α-glucosidase and *Agrobacterium* β-glucosidase. However, the binding affinity of **M10** towards yeast α-glucosidase is actually lower than that of lone quercetin ($IC_{50} = 7$ μM).[16] Comparison of these results with those of previous specificity analyses of mini-MbA and MbA indicated that **M10** was in fact more selective for HPA over the intestinal glucosidases, since mini-MbA and MbA inhibited sucrase-isomaltase and *B. fibrisolvens* α-amylase, respectively.[9,11] This bodes well for the use of **M10** as a selective amylase inhibitor. It also implies that this pharmacophore may have restricted application to other glycosidases.

Inhibitor **M10** demonstrates highly promising HPA inhibition, however the synthetic route that led to its discovery has a number of shortcomings that would hamper its development as a potential pharmaceutical. As such, an alternative approach was devised (Scheme 3). Selective azide reduction of **3 propyl** could be carried out in the presence of **6** to give amide **7**, which could then be globally deprotected to give amine **8**. Treatment of crude amine **8** with **1** then delivered **M10** in 49% yield over four steps, with no purification necessary between steps. This improved procedure delivers **M10** in eight steps from rutin (24% overall yield), with further optimization certainly possible.

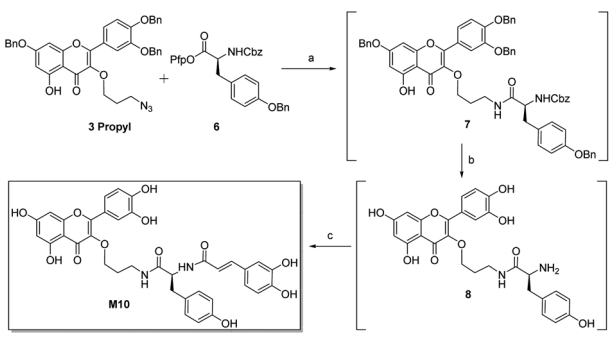

Scheme 3 Improved synthesis of **M10**. (a) Lindlar catalyst (60% w/w), H_2, DMF; (b) pentafluorophenol (4 equiv.), 5% Pd/Al_2O_3 (30% w/w), H_2, DMF; (c) **1** (2 equiv.), Et_3N (2.5 equiv.); 49%.

Conclusions

The synthesis and kinetic analysis of MbA analogues **M01** to **M11** provides new insight into the structural requirements for HPA inhibition. The fact that most of the analogues bound more weakly than mini-MbA highlights the importance of MbA's constrained carbohydrate linker. Despite forming no direct interactions in the active site it appears to pre-stack the flavonol and caffeic acid moieties for optimal interaction. Initial exploration of the effect of incorporation of rigidity into the analogue linkers was achieved with the proline linker of **M06**. This increased potency some 60-fold compared to the non-functionalized glycine linker, with more possibly achievable by freezing out other motions. Affinity enhancement through the acquisition of stabilising interactions was explored through the incorporation of phenolic side chains to recruit some of the hydrophobic and hydrophilic interactions ordinarily developed by the starch substrate in the amylase active site.[17] Indeed the phenolic linkers of **M10** and **M11** take advantage of both such features, rendering the inhibitors six times as potent as mini-MbA, and delivering a higher ligand efficiency than either MbA or mini-MbA (Table S1†). Further, and perhaps surprisingly, the specificity of inhibition is retained despite the reduction in complexity. Thus **M10** and **M11** represent amylase inhibitors that are both much more synthetically accessible and indeed more potent than the mini-MbA that inspired their development. With further optimization of their synthesis underway, pharmacokinetic and efficacy studies with these inhibitors are planned to determine their suitability for therapeutic usage.

Experimental section

Please refer to ESI.†

Conflicts of interest

The University of British Columbia has applied for patent protection on the inhibitors described.

Acknowledgements

We thank Emily Kwan for purification of HPA and Ethan Goddard-Borger for useful discussions at the outset. We acknowledge funding from the Canadian Glycomics Network/Networks of Centres of Excellence (Project DO-2) DOI: 10.13039/501100009056. Portions of this research were carried out at the Stanford Synchrotron Radiation Lightsource, SLAC National Accelerator Laboratory, which is supported by the U.S. Department of Energy, Office of Science, Office of Basic Energy Sciences under Contract No. DE-AC02-76SF00515. The SSRL Structural Molecular Biology Program is supported by the DOE Office of Biological and Environmental Research, and by the NIH, National Institute of General Medical Sciences (including P41GM103393). The contents of this publication are solely the responsibility of the authors and do not necessarily represent the official views of NIGMS or NIH.

References

1 World Health Organization, *Global Report on Diabetes*, 2006, vol. 6.
2 E. Adeghate, P. Schattner and E. Dunn, *Ann. N. Y. Acad. Sci.*, 2006, **1084**, 1; K. G. Alberti and P. Z. Zimmet, *Diabetic Med.*, 1998, **15**(7), 539.
3 A. D. Baron, *Diabetes Res. Clin. Pract.*, 1998, **40**, S51.
4 L. J. Scott and C. M. Spencer, *Drugs*, 2000, **59**(3), 521; K. Kaku, *Expert Opin. Pharmacother.*, 2014, **15**(8), 1181; M. Hanefeld, *J. Diabetes Complicat.*, 1998, **12**(4), 228; P. Phillips, J. Karrasch, R. Scott, D. Wilson and R. Moses, *Diabetes Care*, 2003, **26**(2), 269.
5 R. J. Andrade, M. Lucena, J. L. Vega, M. Torres, F. J. Salmerón, V. Bellot, M. D. García-Escaño and P. Moreno, *Diabetes Care*, 1998, **21**(11), 2029; G. C. Ezeji, T. Inoue, G. Bahtiyar and A. Sacerdote, *BMJ Case Rep.*, 2015, 2015; S. A. Cohen, *Molecular and Cellular Pediatrics*, 2016, **3**(1), 5.
6 G. D. Brayer, Y. Luo and S. G. Withers, *Protein Sci.*, 1995, **4**(9), 1730; E. H. Rydberg, G. Sidhu, H. C. Vo, J. Hewitt, H. C. Côte, Y. Wang, S. Numao, R. T. MacGillivray, C. M. Overall, G. D. Brayer and S. G. Withers, *Protein Sci.*, 1999, **8**(3), 635.
7 S. Numao, I. Damager, C. Li, T. M. Wrodnigg, A. Begum, C. M. Overall, G. D. Brayer and S. G. Withers, *J. Biol. Chem.*, 2004, **279**(46), 48282.
8 G. Horne, F. X. Wilson, J. Tinsley, D. H. Williams and R. Storer, *Drug Discovery Today*, 2011, **16**(3–4), 107.
9 C. A. Tarling, K. Woods, R. Zhang, H. C. Brastianos, G. D. Brayer, R. J. Andersen and S. G. Withers, *ChemBioChem*, 2008, **9**(3), 433.
10 V. G. Yuen, J. Coleman, S. G. Withers, R. J. Andersen, G. D. Brayer, S. Mustafa and J. H. McNeill, *Mol. Cell. Biochem.*, 2016, **411**(1–2), 373.
11 L. K. Williams, X. Zhang, S. Caner, C. Tysoe, N. T. Nguyen, J. Wicki, D. E. Williams, J. Coleman, J. H. McNeill, V. Yuen, R. J. Andersen, S. G. Withers and G. D. Brayer, *Nat. Chem. Biol.*, 2015, **11**(9), 691.
12 Revised K_I for mini-MbA (Fig. S49†).
13 E. Lo Piparo, H. Scheib, N. Frei, G. Williamson, M. Grigorov and C. J. Chou, *J. Med. Chem.*, 2008, **51**(12), 3555.
14 H. Huang, Q. Jia, J. Ma, G. Qin, Y. Chen, Y. Xi, L. Lin, W. Zhu, J. Ding, H. Jiang and H. Liu, *Eur. J. Med. Chem.*, 2009, **44**(5), 1982.
15 M. Green and J. Berman, *Tetrahedron Lett.*, 1990, **31**(41), 2.
16 K. Tadera, Y. Minami, K. Takamatsu and T. Matsuoka, *J. Nutr. Sci. Vitaminol.*, 2006, **52**(2), 149.
17 G. D. Brayer, G. Sidhu, R. Maurus, E. H. Rydberg, C. Braun, Y. Wang, N. T. Nguyen, C. M. Overall and S. G. Withers, *Biochemistry*, 2000, **39**(16), 4778.